

Impact of Distortion of Porphyrins on Axial Coordination in (Porphyrinato)zinc(II) Complexes with Aminopyridines as Axial Ligands

Takahiko Kojima,^{*,[a],[‡]} Tatsuaki Nakanishi,^[a] Tatsuhiko Honda,^[a] Ryosuke Harada,^{[a],[‡],[‡]} Motoo Shiro,^[b] and Shunichi Fukuzumi^{*,[a]}

Keywords: Porphyrinoids / N ligands / Coordination modes / Zinc / Molecular distortion

A series of (porphyrinato)zinc(II) compounds were synthesized with use of 5,10,15,20-tetraphenylporphyrin (H₂TPP), 2,3,5,10,12,13,15,20-octaphenylporphyrin (H₂OPP), and 2,3,5,7,8,10,12,13,15,17,18,20-dodecaphenylporphyrin (H₂DPP). Those compounds form complexes with aniline, pyridine, and 3- and 4-aminopyridines as axial ligands. X-ray crystallography was performed on the complexes with 3-aminopyridine (3-AP) and 4-aminopyridine (4-AP) as axial ligands. 3-Aminopyridine was revealed to bind through the amino group to the Zn(OPP), exhibiting intermolecular π - π interaction between 3-AP and one of the pyrrole rings and intermolecular NH- π interactions of the coordinated amino group with two β -phenyl groups of an adjacent molecule. In solu-

tion, the aminopyridines form a single species at ambient temperature and are assumed to have pyridine coordination through the aromatic pyridine nitrogen atom. Variable-temperature NMR spectroscopy in CD₂Cl₂ indicates that two different species exist at lower temperatures, suggesting that amino-bound complexes of 3-AP can be formed as a metastable species in solution, which is stabilized in the crystal as a result of noncovalent interactions. The binding constants of aminopyridines to the three kinds of (porphyrinato)zinc complexes reveal enhancement of the axial ligation by virtue of the distortion of the porphyrin ring.
(© Wiley-VCH Verlag GmbH & Co. KGaA, 69451 Weinheim, Germany, 2009)

Introduction

Porphyrins, as extended π -conjugated molecules, are known to exhibit planar structures. The introduction of peripheral substituents to the porphyrin skeleton, however, can induce molecular distortion in various manners involving saddling, ruffling, waving, and doming.^[1,2] This porphyrin ring distortion has been suggested to exert certain effects to control the functions of iron centers in heme proteins and heme enzymes in biological systems^[1] and chlorophylls.^[3] Thus, it is important to demonstrate systematic and quantitative treatments of the influence of the porphyrin distortion on the characteristics of porphyrinato complexes.

As a metal center of a metalloporphyrin, the Zn²⁺ ion is also one of the most prevailing metal ions. The Zn²⁺ ion has been known to contribute as a Lewis acid in many kinds of

organic^[4,5] and enzymatic reactions.^[6] The Lewis acidity of the Zn^{II} center can be regulated by the coordination environments and donor sets of the ligands applied. (Porphyrinato)zinc(II) complexes form dominantly five-coordinate square-pyramidal structures.^[7] They have served not only as electron donors in photoinduced electron transfer, but also as building blocks of assemblies. The axial ligation in (porphyrinato)Zn^{II} complexes is not as strong as that in (porphyrinato)transition-metal complexes without d_σ electrons, such as Co^{III} and Cr^{III}.^[8] However, strong donors such as pyridine derivatives can bind fairly strongly to the Zn^{II} center. On the basis of this behavior, the introduction of pyridine compounds as axial ligands of (porphyrinato)Zn^{II} complexes has been examined for various purposes, including template synthesis of multiporphyrin compounds,^[9] self-organization of (porphyrinato)Zn^{II} complexes to form multiporphyrin arrays,^[10] and photoinduced charge separation systems.^[11]

To consider the strength of axial coordination in (porphyrinato)Zn^{II} complexes, we need to pay attention to the Lewis acidity of the Zn^{II} center to construct a stable architecture by taking advantage of the axial ligation. However, no report has appeared to clarify the influence of the distortion of porphyrin ligands in (porphyrinato)Zn^{II} complexes on the Lewis acidity, which can be reflected in the binding constants of axial ligands such as pyridine derivatives.

Thus, we examined the impact of porphyrin distortion on the strength of the axial coordination in (porphyrinato)-

[a] Department of Material and Life Science, Graduate School of Engineering
Osaka University and SORST (JST)
2-1 Yamada-oka, Suita, Osaka 565-0871, Japan
Fax: +81-6-6879-7370
E-mail: kojima@chem.eng.osaka-u.ac.jp
fukuzumi@chem.eng.osaka-u.ac.jp

[b] X-ray Research Laboratory, Rigaku Corporation,
3-9-12 Matsubara, Akishima-shi, Tokyo 196-8666, Japan

[‡] Present address: Department of Chemistry, Graduate School of Pure and Applied Sciences, University of Tsukuba, Tsukuba, Ibaraki 305-8571, Japan
E-mail: kojima@chem.tsukuba.ac.jp

[‡‡] Present address: Center for Future Chemistry, Kyushu University, Moto-oka, Fukuoka 819-0395, Japan

Zn^{II} complexes by adopting tetraphenylporphyrin (H₂TPP), 2,3,5,10,12,13,15,20-octaphenylporphyrin (H₂OPP),^[12] and 2,3,5,7,8,10,12,13,15,17,18,20-dodecaphenylporphyrin (H₂DPP)^[13] as porphyrin ligands showing different extents of distortion and aminopyridines as axial ligands. (Porphyrin)Zn^{II} complexes can be useful probes to evaluate these effects, since Zn^{II} is in a d¹⁰ configuration without change of spin states, and the σ -donating ability of the pyrrole nitrogen atoms in the porphyrins directly reflects on the equilibrium of the axial ligation. Thus, we report herein crystal structures of (aminopyridine)(porphyrinato)Zn^{II} complexes and quantitative evaluation of axial coordination of aminopyridine derivatives in solution to exemplify the influence of porphyrin ring distortion. In the course of our research, we found unusual coordination of 3-aminopyridine, which binds in the crystal to the Zn^{II} center within the OPP²⁻ ligand through the amino nitrogen atom rather than the pyridine nitrogen atom.

Results and Discussion

Crystal Structures of (Aminopyridine)(porphyrinato)zinc Complexes

(Porphyrinato)Zn^{II} complexes with aminopyridine derivatives were synthesized by the reaction of corresponding (porphyrinato)Zn^{II} precursor complexes with aminopyridine in chloroform at room temperature in nearly quantitative yields. Crystal structures of all the complexes were determined by X-ray crystallography. Selected bond lengths [Å] and the deviation of the Zn^{II} center from the least-square planes of the 24 atoms of the porphyrin cores are summarized in Table 1.

Crystal structures of Zn^{II}(TPP) complexes with 3-aminopyridine (3-AP), [Zn(3-AP)(TPP)] (**T3**), and with 4-aminopyridine (4-AP), [Zn(4-AP)(TPP)] (**T4**), are shown as ORTEP drawings in Figures 1 and 2, respectively. **T4** crystallizes in the acentric space group *P*2₁2₁2₁ to give a chiral structure. In both complexes, the aminopyridine derivatives coordinate to the Zn^{II} centers through the aromatic nitrogen atoms. The bond lengths of four Zn–N bonds in the equatorial plane are nearly the same for the two complexes, but the axial bond length [2.083(5) Å] in **T4** is shorter than that [2.128(1) Å] in **T3**. The displacement of the Zn ion from the porphyrin mean plane is larger in **T3** than that in **T4**. In the crystal of **T3**, the amino group of 3-AP exhibits intermolecular NH– π interaction^[14] with the *meso* position

of the adjacent molecule, showing an interatomic distance of 3.48 Å from the opposite side of the 3-AP coordination site relative to the porphyrin plane. No such intermolecular interaction is found for **T4**.

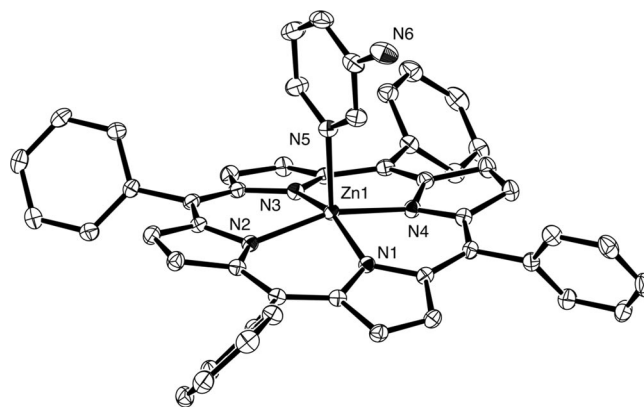


Figure 1. ORTEP drawing of **T3** with selected numbering scheme with thermal ellipsoids at 50% probability. All hydrogen atoms are omitted for clarity.

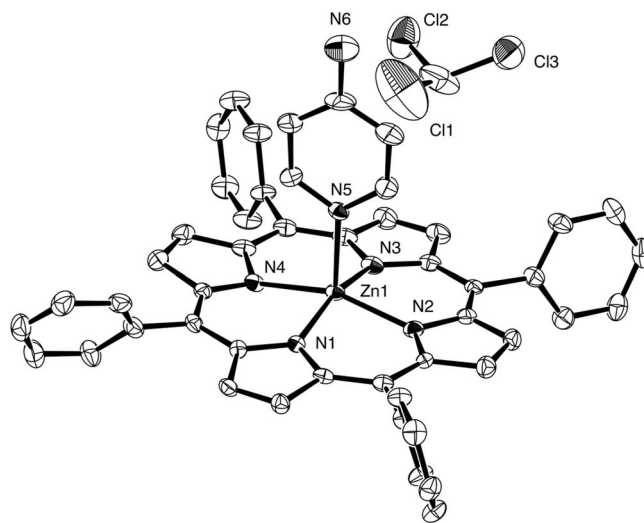


Figure 2. ORTEP drawing of **T4**·CHCl₃ with selected numbering scheme with thermal ellipsoids at 50% probability. All hydrogen atoms are omitted for clarity.

The crystal structures of Zn^{II}(OPP) complexes with 3-AP (**O3**) and 4-AP (**O4**) are depicted in Figures 3 and 4, respectively. To our surprise, they exhibit totally different crystal structures. In sharp contrast to other crystal struc-

Table 1. Selected bond lengths [Å] and displacements [Å] for complexes **T3**, **T4**, **O3**, **O4**, **D3**, and **D4**.

	T3	T4	O3	O4	D3	D4
Zn1–N1	2.080(1)	2.083(4)	2.122(2)	2.034(3)	2.085(3)	2.076(2)
Zn1–N2	2.088(1)	2.079(4)	2.018(2)	2.166(4)	2.077(3)	2.063(3)
Zn1–N3	2.080(1)	2.098(4)	2.133(2)	[a]	2.087(3)	2.111(3)
Zn1–N4	2.071(1)	2.065(4)	2.025(2)	[a]	2.077(3)	2.070(3)
Zn1–N(axial)	2.128(1)	2.083(5)	2.246(2)	2.131(8)	2.127(3)	2.067(3)
Zn displacement	0.4453(3)	0.364	0.327	0.314	0.509	0.471

[a] These values are unavailable owing to the symmetry of the molecule.

tures, the crystal structure of **O3** was revealed to involve the axial ligation of 3-AP at the amino nitrogen atom rather than the pyridine nitrogen atom, as shown in Figure 3(top). The coordination of the amino nitrogen atom in aminopyridine derivatives is unprecedented, allowing us to access a very unique structural motif of the pyridine-bound (porphyrinato)Zn^{II} complex. The 3-AP ligand in **O3** exhibits intramolecular π - π interaction with the pyrrole ring including N1 and displays interatomic distances of 3.21, 3.37, and 3.63 Å. The dihedral angle between the pyridine plane of 3-AP and the pyrrole ring including N1 is estimated to be 22.80° and the intercentroid distance of those two aromatic rings is estimated to be 3.678 Å. In the case of **O4**, 4-AP coordinates to the Zn center through the aromatic pyridine nitrogen atom. In the crystal, the opposite side of the Zn(OPP) moiety to the 4-AP binding site is occupied by two chloroform molecules of crystallization as shown in Figure 4. The molecular orientation of **O4** in the crystal is disordered to give rise to two apparent molecules of 4-AP with a population of 0.5 each.

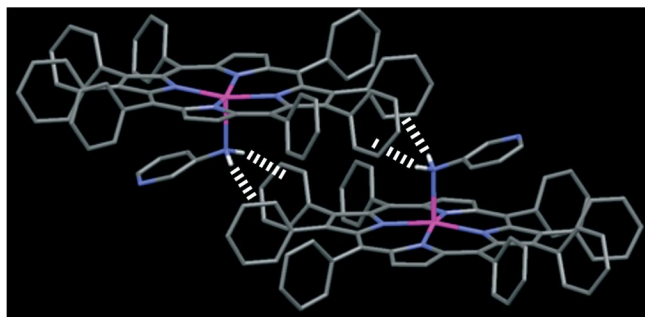
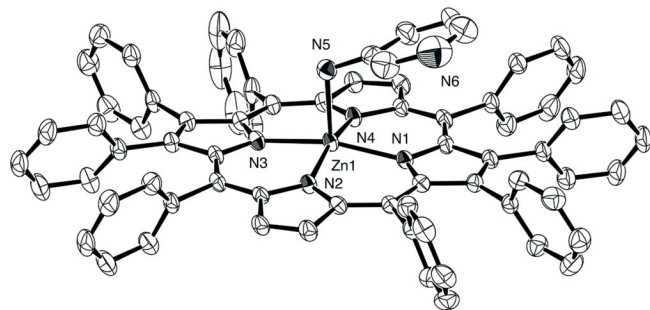


Figure 3. (top) ORTEP drawing of **O3** with selected numbering scheme with thermal ellipsoids at 50% probability. All hydrogen atoms are omitted for clarity. (bottom) Dimeric structure in the crystal with NH- π interactions (dotted white lines). All hydrogen atoms, except amino hydrogen atoms, are omitted for clarity.

In the crystals of both **O3** and **O4**, the amino group of the 3- or 4-aminopyridine ligands is wedged into the cleft made by two β -phenyl groups attached to one of the pyrrole rings of an adjacent molecule to form intermolecular NH- π interactions.^[14] Such interaction found in the crystal of **O3** is demonstrated in Figure 3 (bottom) as dotted lines. As can be seen in Figure 3 (bottom), **O3** forms a dimeric unit by noncovalent interactions. The interatomic distances (N \cdots C) are 3.52 and 3.35 Å for **O3** and 3.34 Å and 3.39 Å for **O4**.

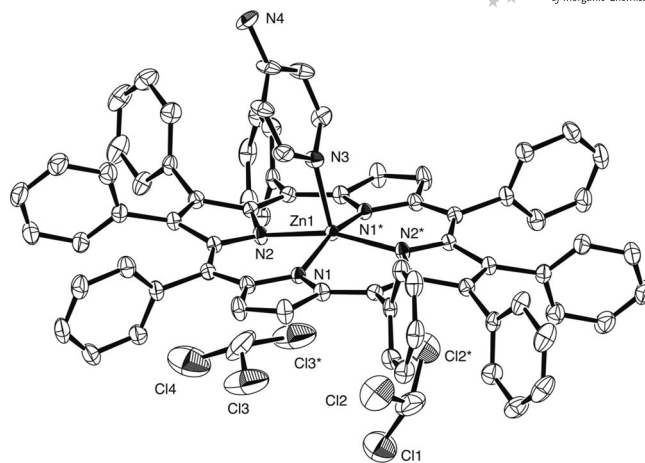


Figure 4. ORTEP drawing of **O4**·2CHCl₃ with selected numbering scheme with thermal ellipsoids at 50% probability. All hydrogen atoms are omitted for clarity.

The synthesis of **D3** was somewhat different from those of the other complexes because of its low solubility in CH₂Cl₂. Crystal structures of the Zn(DPP) complexes with 3-AP (**D3**) and 4-AP (**D4**) are presented in Figures 5 and 6, respectively. In each case, the DPP ligand exhibits severe saddle distortion, which is typical for this ligand. In both cases, the aminopyridine ligands coordinate to the Zn^{II} centers through the aromatic nitrogen atoms. In the crystal of **D4**, the amino group of the 4-AP ligand forms NH- π interactions with pyrrole nitrogen atoms of an adjacent molecule, showing interatomic distances of 3.05 and 3.45 Å from the opposite side of the 4-AP coordination site relative to the porphyrin plane. In contrast, no such intermolecular interactions are recognized for the amino groups of **D3** in the crystal.

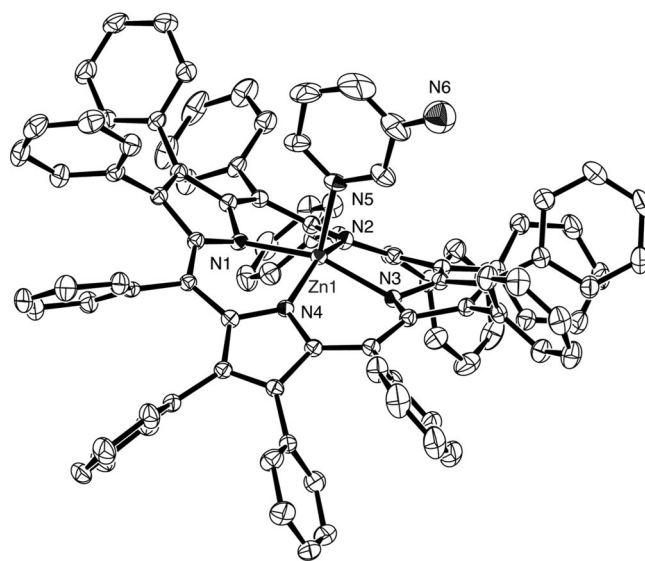


Figure 5. ORTEP drawing of **D3** with selected numbering scheme with thermal ellipsoids at 50% probability. All hydrogen atoms are omitted for clarity.

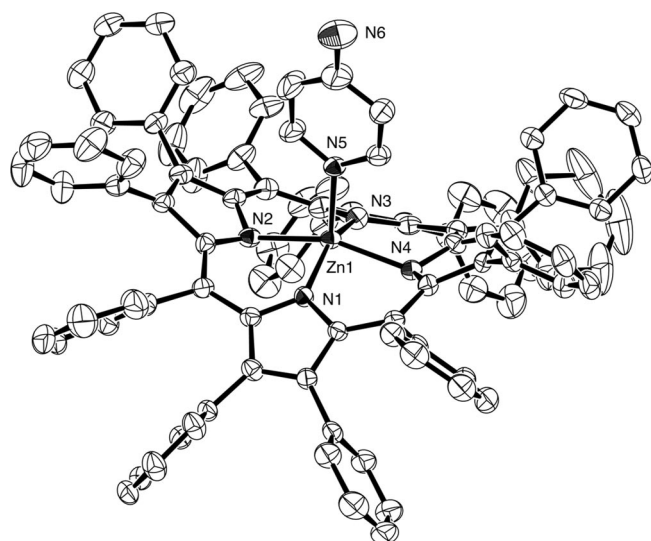


Figure 6. ORTEP drawing of **D4** with selected numbering scheme with thermal ellipsoids at 50% probability. All hydrogen atoms are omitted for clarity.

As a general feature of the structures presented above, the bonds of the axial ligand for 3-AP are longer than those for 4-AP, as listed in Table 1. This difference results from the stronger basicity of the pyridine nitrogen atom in 4-AP than that in 3-AP [$pK_a(3\text{-AP}) = 6.04$ and $pK_a(4\text{-AP}) = 9.11$ at 25 °C].^[15] As for the porphyrinato ligands, the order of the bond lengths for the axial ligands is DPP < TPP < OPP. This result is consistent with the order of the displacement of the Zn²⁺ ion from the porphyrinato mean plane. The displacement of the Zn²⁺ ion is the largest in **D3** (0.509 Å) and the smallest in **O4** (0.314 Å). Those values listed in Table 1 are larger than that observed in [Zn(CH₃CN)(DPP)] [0.233(1) Å].^[16] As the tendency of the Zn^{II} displacements, coordination of 3-AP causes larger displacement than that of 4-AP.

The crystal structure determination described above allowed us to estimate the distortion of the porphyrinato rings in the complexes. The displacements of the 24 atoms of the porphyrinato core from the mean porphyrinato plane of each complex are given in Figure 7. In the cases of **T3** and **T4**, the TPP ligand exhibit slight saddle distortion as represented by the signs of displacements at the β -positions of the pyrrole rings: Two of those *trans* to each other show the same directions of displacements. The DPP complexes **D3** and **D4** exhibit larger saddle distortion than that found in the TPP complexes, and the saddle distortion is much larger than that observed in [Zn(CH₃CN)(DPP)].^[16] In the case of the OPP ligand, **O3** and **O4** show smaller distortion than that found in the TPP complexes and different distortions from each other: The OPP ligand is almost planar but slightly saddle-distorted in **O3**; the OPP ligand in **O4** exhibits a slight wave distortion. We also found a similar extent of such wave distortion in the crystal structure of [Cr(OPP)(piperidine)₂ClO₄].^[17]

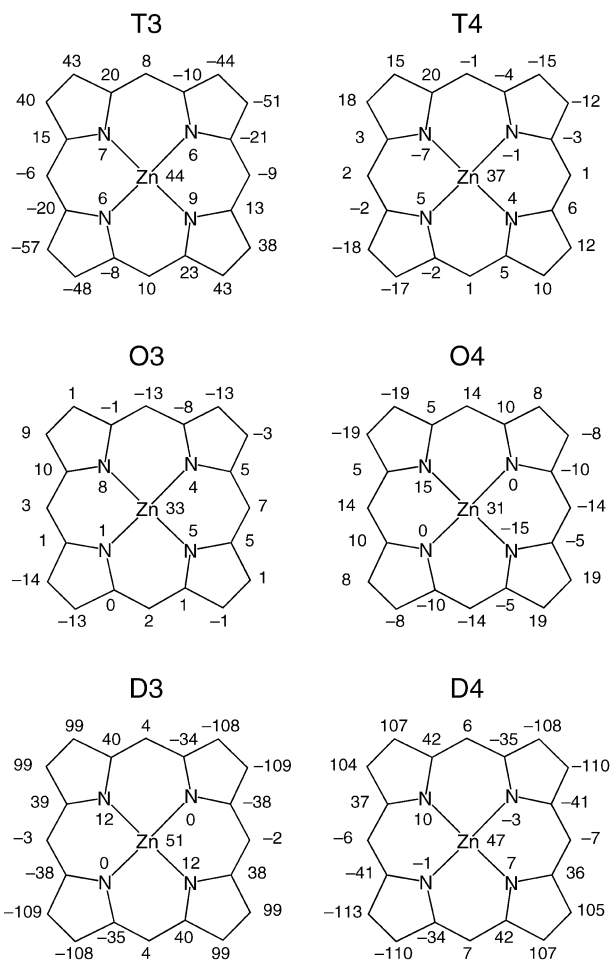


Figure 7. Displacements of atoms from the mean porphyrinato plane (in units of 0.01 Å).

Coordination of Aminopyridine Ligands in CH₂Cl₂

To examine the structures of the complexes in solution, we measured variable-temperature ¹H NMR spectra in CD₂Cl₂. However, the solubility of **D3** was poor and did not allow us to obtain its ¹H NMR spectrum. The (porphyrinato)Zn complexes of 3-AP and 4-AP exhibit the same spectral pattern for signals due to the porphyrinato rings in all cases, indicating that the axial ligands undergo a fast binding/dissociation equilibrium on the NMR timescale at room temperature. By lowering the temperature to -90 °C, we could observe another set of signals, which could be assigned to the ligated species. The variable-temperature ¹H NMR spectra of **T4** are shown in Figure 8 as a typical example. As the temperature is lowered, signals due to coordinated 4-AP sharpen and are observed clearly. A doublet assigned to the 2-H and the 6-H atoms emerge at $\delta = 1.84$ ppm (-90 °C) with a large upfield shift caused by strong shielding derived from the porphyrinato π -electron ring current, indicating the coordination of the pyridine nitrogen atom in 4-AP. Another doublet ascribed to the 3-H and the 5-H atoms is observed at $\delta = 4.58$ ppm (-90 °C) with less shielding by the porphyrin ring current. In addition, a broad singlet at $\delta = 3.42$ ppm (-90 °C) is assigned

to the NH protons of the amino group of 4-AP. In the case of **O3**, its NMR spectrum at $-90\text{ }^{\circ}\text{C}$ exhibits a singlet assigned to the 2-H atom at $\delta = 1.70\text{ ppm}$ and a doublet due to the 6-H atom at $\delta = 1.91\text{ ppm}$ with large upfield shift. This result indicates that 3-AP coordinates in solution through the pyridine nitrogen atom rather than the amino nitrogen atom, which is in sharp contrast to its crystal structure depicted in Figure 3.

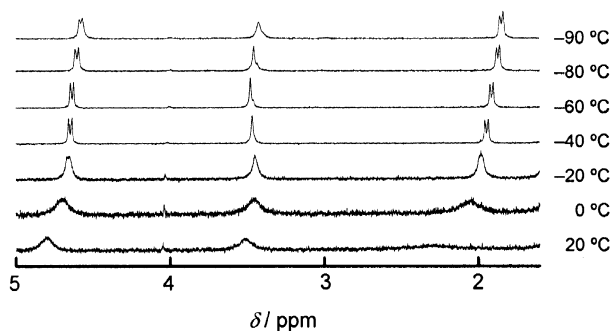


Figure 8. Variable-temperature ^1H NMR spectra for **T4** in CD_2Cl_2 .

To determine binding constants (K_{bind}) of aniline, pyridine, 3-AP, and 4-AP to (porphyrinato) Zn^{II} complexes, we conducted spectroscopic titrations in CH_2Cl_2 at a concentration of the (porphyrinato) Zn complexes of $3.0 \times 10^{-5}\text{ M}$ at room temperature. The spectral change in the course of the spectroscopic titration is depicted in Figure 9 for **D4** as a representative example. In all cases, the axial coordination of the ligands induced redshifts in the Soret and Q bands in the absorption spectra. The binding constants obtained are summarized in Table 2.

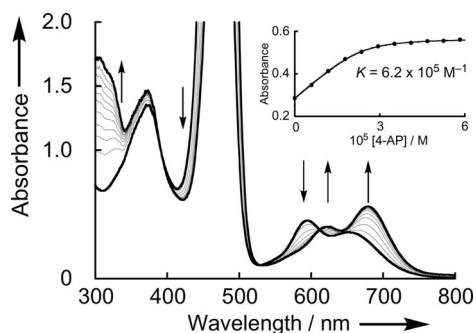


Figure 9. UV/Vis spectral change of $\text{Zn}(\text{DPP})$ ($3.0 \times 10^{-5}\text{ M}$) upon addition of various concentrations of 4-AP (0 , 6×10^{-6} , 1.2×10^{-5} , 1.8×10^{-5} , 2.4×10^{-5} , 3.0×10^{-5} , 3.6×10^{-5} , 4.2×10^{-5} , 4.8×10^{-5} , 5.4×10^{-5} , and $6.0 \times 10^{-5}\text{ M}$) in CH_2Cl_2 at room temperature. Inset: absorption changes at 680 nm .

As an overview, the binding constants are in the order aniline $<$ pyridine $<$ 3-AP $<$ 4-AP for the axial ligands examined and $\text{TPP}^{2-} <$ $\text{OPP}^{2-} <$ DPP^{2-} for the porphyrinato ligands. The order of the binding constants depending on the axial ligands is consistent with that of their $\text{p}K_{\text{a}}$ values: aniline (4.87) $<$ pyridine (5.23) $<$ 3-AP (6.04) $<$ 4-AP (9.11), at $25\text{ }^{\circ}\text{C}$.^[13] Linear correlations of the $\log K_{\text{bind}}$ values relative to the $\text{p}K_{\text{a}}$ values were observed as shown in Figure 10. A similar tendency has been reported for $\text{Zn}(\text{TPP})$ complexes.^[15] The slope of the plot ($+0.236$) for the $\text{Zn}(\text{TPP})$ complexes is consistent with that reported previously,^[18] but the gradients for the $\text{Zn}(\text{OPP})$ ($+0.314$) and $\text{Zn}(\text{DPP})$ ($+0.268$) complexes are different from that of $\text{Zn}(\text{TPP})$ complexes. Although the theoretical background of the gradients of those relationships has not yet been established, our results indicate that the slope is not necessarily the same but that it depends on the porphyrin involved.

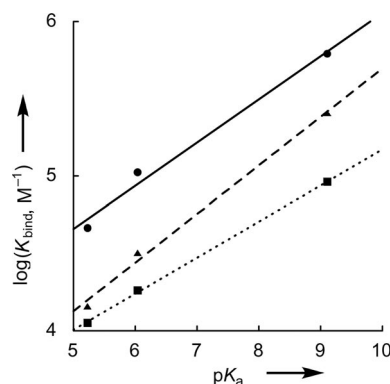


Figure 10. Relationship between the logarithm of binding constants of pyridine derivatives and their $\text{p}K_{\text{a}}$ values (pyridine, 5.23 ; 3-AP, 6.04 ; 4-AP, 9.11): $\text{Zn}(\text{TPP})$ (■), $\text{Zn}(\text{OPP})$ (▲), and $\text{Zn}(\text{DPP})$ (●).

We performed DFT calculations to clarify the influence of the distortion of the porphyrinato ligands on the binding constants. The structure optimizations were made on four-coordinate $\text{Zn}(\text{TPP})$, $\text{Zn}(\text{OPP})$, and $\text{Zn}(\text{DPP})$ structures based on the crystal structures of $[\text{Zn}(4\text{-AP})(\text{TPP})]$, $[\text{Zn}(4\text{-AP})(\text{OPP})]$, and $[\text{Zn}(\text{CH}_3\text{CN})(\text{DPP})]$. The degrees of distortion of the porphyrinato ligands were estimated by root-mean-square out-of-plane displacement (ΔRMS), which is defined by Equation (1):^[19]

$$\Delta\text{RMS} = \sqrt{\frac{1}{24} \sum_{i=1}^{24} \delta_i^2} \quad (1)$$

where δ_i is the orthogonal displacement of atom i in the macrocycle from the mean plane including all 24 atoms of the porphyrinato macrocycle. As can be seen in Figure 11,

Table 2. Binding constants of various axial ligands to (porphyrinato) Zn^{II} complexes.^[a]

	ΔRMS [\AA]	Aniline	Pyridine	3-AP	4-AP
$\text{Zn}(\text{TPP})$	0.06	$(1.6 \pm 0.1) \times 10^2$	$(1.1 \pm 0.1) \times 10^4$	$(1.8 \pm 0.1) \times 10^4$	$(9.2 \pm 0.4) \times 10^4$
$\text{Zn}(\text{OPP})$	0.44	$(1.9 \pm 0.5) \times 10^2$	$(1.4 \pm 0.2) \times 10^4$	$(3.2 \pm 0.5) \times 10^4$	$(2.5 \pm 0.2) \times 10^5$
$\text{Zn}(\text{DPP})$	0.57	$(3.2 \pm 0.4) \times 10^2$	$(4.6 \pm 0.2) \times 10^4$	$(1.1 \pm 0.0) \times 10^5$	$(6.2 \pm 0.0) \times 10^5$

[a] Measured in CH_2Cl_2 at room temperature. $[(\text{porphyrinato})\text{Zn}] = 3.0 \times 10^{-5}\text{ M}$.

the binding constants are proportional to the ΔRMS values for pyridine, 3-AP, and 4-AP in every porphyrinato system employed here. These results indicate that the degree of porphyrin distortion can regulate the strength of the axial coordination. The ring distortion should enforce lone pairs of nitrogen atoms in the pyrrole moieties to direct out of plane, and this ill-direction of the lone pairs can weaken the interaction between the Zn^{II} center and the nitrogen lone pairs to enhance the Lewis acidity of the Zn^{II} center. Thus, the more the porphyrinato ring is distorted as reflected in a larger ΔRMS value, the stronger the Lewis acidity of the Zn^{II} center becomes.

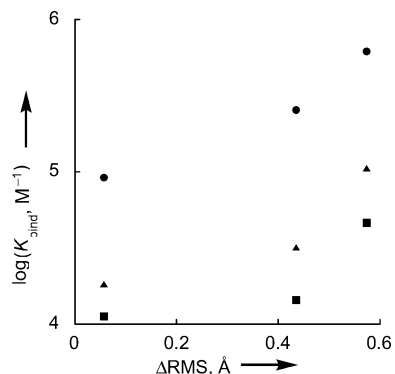


Figure 11. Correlations between the logarithm of binding constants of pyridine derivatives and root-mean-square out-of-plane displacements of porphyrin ligands [Zn(TPP), 0.06; Zn(OPP), 0.44; Zn(DPP), 0.57]: pyridine (■), 3-AP (▲), and 4-AP (●).

Conclusions

We have determined a series of crystal structures of (porphyrinato)Zn^{II} complexes with aminopyridine isomers and demonstrated a novel coordination mode of 3-aminopyridine involving coordination of the amino nitrogen atom rather than the more σ -donating pyridine nitrogen atom. The Zn^{II} complexes of TPP²⁻, OPP²⁻, and DPP²⁻ showed different degrees of distortion of the porphyrinato rings. Among them, the DPP²⁻ ligand exhibited the largest non-planarity as a saddle distortion and the largest displacement of the Zn²⁺ ion from the porphyrinato mean plane. In solution, NMR measurements revealed that all the aminopyridine derivatives underwent coordination of the aromatic nitrogen atom in all porphyrinato systems at room temperature. The strength of binding of these ligands is regulated not only by the basicity of the pyridine nitrogen atom to control the ability of σ -donation but also the distortion of the porphyrinato ligands to regulate the Lewis acidity of the metal center.

Experimental Section

Materials: H₂OPP was prepared by a cross-coupling reaction between phenylboronic acid and 2,3,12,13-tetrabromo-5,10,15,20-tetraphenylporphyrin according to the procedures described by Chan et al.^[12] Zn(TPP) was synthesized by the reaction of H₂TPP with

zinc acetate. Other chemicals were purchased from commercial sources and used without further purification.

Zn(OPP): H₂OPP (100 mg, 0.109 mmol) and Zn(AcO)₂·2H₂O (239 mg, 1.09 mmol) were heated at reflux in CHCl₃/MeOH (5:3, v/v; 80 mL) for 2 h. The solvents were evaporated under reduced pressure. The residue was dissolved in a minimum amount of CHCl₃ and chromatographed on a silica gel column by using CHCl₃ as the eluent. The first red fraction was collected, and the solvent was evaporated. The product was recrystallized from CHCl₃/hexane to afford a purple crystalline solid. Yield: 0.104 g (97%). ¹H NMR (270 MHz, CDCl₃, 298 K): δ = 8.50 (s, 4 H, β -H), 7.76 (d, 8 H, *meso*-phenyl *o*-H), 7.20 (m, 12 H, *meso*-phenyl *m,p*-H), 7.03 (d, 8 H, β -phenyl *o*-H), 6.89 (m, 12 H, β -phenyl *m*- and *p*-H) ppm. UV/Vis (CH₂Cl₂): λ_{max} = 430, 558 nm.

[Zn(3-AP)(TPP)] (T3): Zn(TPP) (20 mg, 0.030 mmol) and 3-aminopyridine (3.4 mg, 0.036 mmol) were dissolved in CHCl₃/hexane (2:3, v/v; 15 mL). A purple crystalline solid was obtained by slow concentration of the solution. Yield: 21 mg (91%). C₄₉H₃₄N₆Zn·0.5H₂O (781.25): calcd. C 75.33, H 4.51, N 10.75; found C 75.20, H 4.48, N 10.79. ¹H NMR (300 MHz, CD₂Cl₂, 233 K): δ = 8.86 (s, 8 H, β -H), 8.17 (s, 8 H, phenyl *o*-H), 7.73 (m, 12 H, phenyl *m-, p*-H), 5.69 (d, *J* = 8 Hz 1 H, pyridyl 4-H), 2.54 (s, 2 H, NH₂), 1.72, 1.68 (d, *J* = 11 Hz 2 H, 6-H and 2-H) ppm. The signal of the pyridyl 5-H proton overlapped with the residual solvent peak at δ = 5.32 ppm. UV/Vis (CH₂Cl₂): λ_{max} = 428, 563, 603 nm.

[Zn(4-AP)(TPP)] (T4): Zn(TPP) (20 mg, 0.030 mmol) and 4-aminopyridine (3.4 mg, 0.036 mmol) were dissolved in CHCl₃/hexane (2:3, v/v; 15 mL). A purple crystalline solid was obtained by slow concentration of the solution. Yield: 23 mg (98%). C₄₉H₃₄N₆Zn·0.5CHCl₃·1.5H₂O (858.95): calcd. C 69.21, H 4.40, N 9.78; found C 68.99, H 4.09, N 9.69. ¹H NMR (300 MHz, CD₂Cl₂, 233 K): δ = 8.85 (s, 8 H, β -H), 8.17 (d, *J* = 7 Hz 8 H, phenyl *o*-H), 7.74 (m, 12 H, phenyl *m-, p*-H), 4.63 (d, *J* = 7 Hz, 2 H, pyridyl *m*-H), 3.48 (s, 2 H, NH), 1.91 (d, *J* = 6 Hz, 2 H, pyridyl *o*-H) ppm. UV/Vis (CH₂Cl₂): λ_{max} = 428, 564, 604 nm.

[Zn(3-AP)(OPP)] (O3): Zn(OPP) (30 mg, 0.030 mmol) and 3-aminopyridine (3.4 mg, 0.036 mmol) were dissolved in CHCl₃/hexane (1:1, v/v; 20 mL). A purple crystalline solid was obtained by slow concentration of the solution. Yield: 27 mg (84%). C₇₃H₅₀N₆Zn·2H₂O (1112.66): calcd. C 78.80, H 4.89, N 7.55; found C 78.65, H 4.92, N 7.81. ¹H NMR (300 MHz, CD₂Cl₂, 233 K): δ = 8.42 (s, 4 H, β -H), 7.78 (d, *J* = 12 Hz, 8 H, *meso*-phenyl *o*-H), 7.19 (m, 12 H, *meso*-phenyl *m-, p*-H), 6.96 (d, *J* = 5 Hz, 8 H, β -phenyl *o*-H), 6.85 (m, 12 H, β -phenyl *m-, p*-H), 5.76 (d, *J* = 8 Hz, 1 H, pyridyl 4-H), 5.48 (t, *J* = 7 Hz, 1 H, pyridyl 5-H), 2.26 (s, 2 H, NH), 1.99 (d, 1 H, pyridyl 6-H), 1.84 (s, 1 H, pyridyl 2-H) ppm. UV/Vis (CH₂Cl₂): λ_{max} = 443, 575, 626 nm.

[Zn(4-AP)(OPP)] (O4): Zn(OPP) (30 mg, 0.030 mmol) and 4-aminopyridine (3.4 mg, 0.036 mmol) were dissolved in CHCl₃/hexane (1:1, v/v; 20 mL). A purple crystalline solid was obtained by slow concentration of the solution. Yield: 31 mg (97%). C₇₃H₅₀N₆Zn·1.5CHCl₃·2.5H₂O (1300.74): calcd. C 68.79, H 4.38, N 6.46; found C 68.78, H 4.23, N 6.43. ¹H NMR (300 MHz, CD₂Cl₂, 233 K): δ = 8.42 (s, 4 H, β -H), 7.80 (ABq, *J*_{AB} = 15 Hz, 8 H, *meso*-phenyl *o*-H), 7.19 (m, 12 H, *meso*-phenyl *m-, p*-H), 7.05 (d, *J* = 5 Hz, 8 H, β -phenyl *o*-H), 6.84 (m, 12 H, β -phenyl *m,p*-H), 4.82 (d, *J* = 6 Hz, 2 H, pyridyl *m*-H), 3.63 (s, 2 H, NH), 2.15 (d, *J* = 6 Hz, 2 H, pyridyl *o*-H) ppm. UV/Vis (CH₂Cl₂): λ_{max} = 443, 576, 626 nm.

Table 3. Crystallographic data for complexes **T3**, **T4**, **O3**, **O4**, **D3**, and **D4**.

	T3	T4	O3	O4	D3	D4
Empirical formula	C ₄₉ H ₃₄ N ₆ Zn	C ₅₀ H ₃₅ Cl ₃ N ₆ Zn	C ₇₃ H ₅₀ N ₆ Zn	C ₇₅ H ₅₂ Cl ₆ N ₆ Zn	C ₉₇ H ₆₆ N ₆ Zn	C ₉₂ H ₆₄ N ₆ Zn
Formula mass	772.23	891.61	1076.62	1315.37	1380.93	1318.86
Crystal system	monoclinic	orthorhombic	monoclinic	monoclinic	triclinic	monoclinic
Space group	<i>P</i> ₂ ₁ / <i>n</i>	<i>P</i> ₂ ₁ 2 ₁ 2 ₁	<i>P</i> ₂ ₁ / <i>c</i>	<i>C</i> 2/ <i>m</i>	<i>P</i> $\bar{1}$	<i>P</i> ₂ ₁ / <i>a</i>
<i>a</i> [Å]	14.5281(17)	9.690(3)	17.573(1)	13.6586(16)	8.4808(19)	18.198(3)
<i>b</i> [Å]	17.209(2)	17.667(5)	12.9073(6)	20.8378(14)	17.858(4)	28.373(5)
<i>c</i> [Å]	14.7967(18)	25.200(3)	24.716(2)	11.0276(9)	17.858(4)	18.424(3)
α [°]	90	90	90	90	83.901(5)	90
β [°]	93.770(6)	90	106.200(3)	100.287(4)	81.562(5)	110.855(3)
γ [°]	90	90	90	90	76.306(5)	90
<i>V</i> [Å ³]	3691.5(8)	4314.0(19)	5383.5(6)	3088.2(5)	4172.8(17)	8889(3)
<i>Z</i>	4	4	4	2	2	4
<i>T</i> [K]	133	133	183.1	123.1	123.1	123.1
<i>D</i> _{calcd.} [g cm ⁻³]	1.389	1.373	1.328	1.414	1.099	0.985
μ [mm ⁻¹]	0.711	0.798	0.509	0.708	0.342	0.318
Total reflections	53232	43114	12236	10272	32971	84930
Unique reflections	8441	9874	12198	2859	17072	20120
Observed reflections [<i>I</i> > 2 σ (<i>I</i>)]	7318	8057	9424	2766	13466	15222
Parameters	506	554	721	250	1104	939
Final <i>R</i> indices ^[a]	<i>R</i> ₁ = 0.0310 <i>wR</i> ₂ = 0.0872	<i>R</i> ₁ = 0.0875 <i>wR</i> ₂ = 0.2193	<i>R</i> ₁ = 0.0579 <i>wR</i> ₂ = 0.1799	<i>R</i> ₁ = 0.0721 <i>wR</i> ₂ = 0.1817	<i>R</i> ₁ = 0.0624 <i>wR</i> ₂ = 0.1949	<i>R</i> ₁ = 0.0836 ^[b] <i>wR</i> ₂ = 0.2298 ^[b]
Largest difference peak/hole [e Å ⁻³]	0.38/−0.36	1.55/−1.13	1.52/−0.57	0.87/−0.58	0.93/−0.53	1.27/−0.59
Goodness of fit on <i>F</i> ²	1.114	1.032	1.000	1.087	1.171	1.083

[a] *R*₁ for *I* > 2 σ (*I*) and *wR*₂ for all data. [b] The SQUEEZE program was applied.

[Zn(3-AP)(DPP)] (D3): To a solution of [Zn(DPP)] (30 mg, 0.023 mmol) in CH₂Cl₂ (2 mL), was added a solution of 3-aminopyridine (7.5 mg, 0.080 mmol) in CH₃CN (1 mL) to obtain a two-layered solution. In the course of the diffusion of the CH₃CN solution, single crystals of **D3** were obtained. Yield: 22 mg (82%). C₉₇H₆₆N₆Zn·3H₂O (1435.07): calcd. C 81.19, H 5.06, N 5.86; found C 81.40, H 5.01, N 5.55. UV/Vis (CH₂Cl₂): λ_{max} = 478, 619, 675 nm.

[Zn(DPP)(4-AP)] (D4): To a solution of [Zn(DPP)] (30 mg, 0.023 mmol) in toluene (2 mL), was added a solution of 4-aminopyridine (7.5 mg, 0.080 mmol) in CH₃OH (0.3 mL). Vapor diffusion of hexane into the mixed solution gave single crystals of **D4**. Yield: 20 mg (73%). C₉₇H₆₆N₆Zn·3H₂O (1435.07): C 81.19, H 5.06, N 5.86; found C 81.20, H 5.12, N 6.02. UV/Vis (CH₂Cl₂): λ_{max} = 478, 621, 676 nm.

Physical Measurements: Absorption spectra were recorded with a Jasco V-570 spectrophotometer in CH₂Cl₂ in the range of 200–800 nm at room temperature. ¹H NMR spectra in CD₂Cl₂ were measured with JEOL GX-400 (400 MHz), EX-270 (270 MHz), and A-300 (300 MHz) spectrometers. Variable-temperature NMR spectra were obtained with a JEOL A-300 spectrometer.

Electrochemical Measurements: Cyclic voltammograms were measured in CH₂Cl₂ (0.1 M [*n*Bu₄N]PF₆ as an electrolyte) at room temperature with a BAS model ALS-720 potentiostat by using a platinum wire as a counter electrode, a glassy carbon electrode as a working electrode, and Ag/AgNO₃ as a reference electrode.

DFT Calculations: All DFT calculations were performed at the B3LYP/6-31G(d) level of theory with use of Gaussian 03^[20] on a 32-processor QuantumCubeTM. Initial structures of four-coordinate [Zn(TPP)], [Zn(OPP)], and [Zn(DPP)] were constructed on the basis of the crystal structures of **T4**, **O4**, and [Zn(CH₃CN)(DPP)].

X-ray Crystallography: Single crystals were mounted on glass capillaries with silicon grease. Diffraction data for **T3** and **T4** were collected with a Rigaku R-AXIS RAPID Imaging Plate dif-

fractometer with monochromated Mo-*K*_α (λ = 0.7107 Å) radiation at −140 °C up to $2\theta_{\text{max}}$ = 55.0°. Diffraction data for **O3–D4** were obtained with a Rigaku Mercury CCD area detector with monochromated Mo-*K*_α (λ = 0.7107 Å) radiation at −90 °C up to $2\theta_{\text{max}}$ = 55.0°. In the case of **O4**, the data used for the structure refinement was limited to $2\theta_{\text{max}}$ = 51.0° because of the quality of the crystal. The structures were solved by direct methods and expanded by using Fourier techniques. All non-hydrogen atoms were refined anisotropically. Refinement was carried out with full-matrix least squares on *F* including anomalous dispersion effects. All calculations were performed by using the Crystal Structure crystallographic software package,^[21] and structure refinements were made by using SHELX-97.^[22] Crystallographic data are summarized in Table 3. For the structure refinement for **D4**, the SQUEEZE program^[23] was applied to improve the refinement by subtracting severely disordered solvent molecules of crystallization (CH₂Cl₂ and *n*-hexane) from the diffraction pattern. CCDC-706362 (**T3**), -706363 (**T4**), -706364 (**O3**), -706365 (**O4**), -706366 (**D3**), and -706367 (**D4**) contain the supplementary crystallographic data for this paper. These data can be obtained free of charge from The Cambridge Crystallographic Data Centre via www.ccdc.cam.ac.uk/data_request/cif.

Acknowledgments

This work was supported by Grants-in-Aid (Nos. 18033033, 19205019, and 19750034), and a Global COE program, “the Global Education and Research Center for Bio-Environmental Chemistry” from the Ministry of Education, Culture, Sports, Science and Technology, Japan, is gratefully acknowledged. T. N. was supported by a JSPS predoctoral fellowship (No. A208410), for which thanks are due. We also appreciate support from the Japan Science and Technology Agency (JST) through the “Potentiality verification stage” program.

- [1] J. A. Shelnut, X.-Z. Song, J.-G. Ma, S.-L. Jia, W. Jensen, C. J. Medforth, *Chem. Soc. Rev.* **1998**, *27*, 31–41.
- [2] R. Harada, Y. Matsuda, H. Okawa, R. Matsumoto, S. Yamachi, T. Kojima, *Inorg. Chim. Acta* **2005**, *358*, 2489–2500.
- [3] K. M. Barkigia, L. Chantranupong, K. M. Smith, J. Fajer, *J. Am. Chem. Soc.* **1988**, *110*, 7566–7567.
- [4] Zn^{II} salts as Lewis acid catalysts: a) M. T. Reetz, *Angew. Chem. Int. Ed. Engl.* **1982**, *21*, 96–108; b) A. Wang, H. Jiang, *J. Am. Chem. Soc.* **2008**, *130*, 5030–5031; c) Y. Li, H. Zou, J. Gong, J. Xiang, T. Luo, J. Quan, G. Wang, Z. Yang, *Org. Lett.* **2007**, *9*, 4057–4060; d) Y. Motoyama, H. Nishiyama, in *Lewis Acids in Organic Synthesis* (Ed.: H. Yamamoto), Wiley-VCH, Weinheim, **2000**, pp. 59–88.
- [5] For a quantitative measure of the Lewis acidity of Zn^{II} salts, see: a) S. Fukuzumi, K. Ohkubo, *Chem. Eur. J.* **2000**, *6*, 4532–4535; b) H. Ohtsu, S. Fukuzumi, *Chem. Lett.* **2001**, 920–921; c) S. Fukuzumi, K. Ohkubo, *J. Am. Chem. Soc.* **2002**, *124*, 10270–10271; d) K. Ohkubo, S. C. Menon, A. Orita, J. Otera, S. Fukuzumi, *J. Org. Chem.* **2003**, *68*, 4720–4726.
- [6] Zn-containing enzymes: S. J. Lippard, J. M. Berg, *Principles of Bioinorganic Chemistry*, University Science Books, Mill Valley, **1994**, pp. 257–281.
- [7] a) D. M. Collins, J. L. Hoard, *J. Am. Chem. Soc.* **1970**, *92*, 3761–3771; b) M. L. Bobrik, F. A. Walker, *Inorg. Chem.* **1980**, *19*, 3383–3390; c) D. L. Cullen, E. F. Meyer Jr, *Acta Crystallogr., Sect. B* **1976**, *32*, 2259–2269; K. Hatano, K. Kawasaki, S. Munakata, Y. Iitaka, *Bull. Chem. Soc. Jpn.* **1987**, *60*, 1985–1992; B. Cheng, W. R. Scheidt, *Inorg. Chim. Acta* **1995**, *237*, 5–11; d) Y. Deng, C. K. Chang, D. G. Nocera, *Angew. Chem. Int. Ed.* **2000**, *39*, 1066–1068.
- [8] J. E. Huheey, E. A. Keiter, R. L. Keiter *Inorganic Chemistry*, 4th ed., Harper Collins College Publishers, New York, **1993**, pp. 547–550.
- [9] a) I. Bouamaied, T. Coskun, E. Stulz, *Struct. Bonding (Berlin)* **2006**, *121*, 1–47; b) Y. Kobuke, *Struct. Bonding (Berlin)* **2006**, *121*, 49–104; c) S. Anderson, H. L. Anderson, J. K. M. Sanders, *Acc. Chem. Res.* **1993**, *26*, 469–475.
- [10] a) C. A. Hunter, L. D. Sarson, *Angew. Chem. Int. Ed. Engl.* **1994**, *33*, 2313–2316; b) R. T. Stibrany, J. Vasudevan, S. Knapp, J. A. Potenza, T. Emge, H. J. Schugar, *J. Am. Chem. Soc.* **1996**, *118*, 3980–3981; c) Y. Diskin-Posner, S. Dahal, I. Goldberg, *Angew. Chem. Int. Ed.* **2000**, *39*, 1288–1292; d) A. Camara-Campos, C. A. Hunter, S. Thomas, *Proc. Natl. Acad. Sci. USA* **2006**, *103*, 3034–3038.
- [11] a) S. Fukuzumi, *Bull. Chem. Soc. Jpn.* **2006**, *79*, 177–195; b) F. D'Souza, O. Ito, *Coord. Chem. Rev.* **2005**, *205*, 1410–1422 and references cited therein.
- [12] K. S. Chan, X. Zhou, B.-S. Luo, T. C. W. Mak, *J. Chem. Soc., Chem. Commun.* **1994**, 271–272.
- [13] a) C. J. Medforth, M. O. Senge, K. M. Smith, L. D. Sparks, J. A. Shelnut, *J. Am. Chem. Soc.* **1992**, *114*, 9859–9869; b) C.-J. Liu, W.-Y. Yu, S.-M. Peng, T. C. W. Mak, C.-M. Che, *J. Chem. Soc., Dalton Trans.* **1998**, *11*, 1805–1812.
- [14] G. R. Desiraju, T. Steiner, *The Weak Hydrogen Bond*, Oxford University Press, New York, **1999**, chapter 3.
- [15] *Handbook of Chemistry and Physics*, 82nd ed. (Ed.: D. R. Lide), CRC Press, Boca Raton, **2001**, pp. 8–48.
- [16] T. Kojima, R. Harada, *Acta Crystallogr., Sect. E* **2004**, *60*, m1097–m1099.
- [17] R. Harada, Y. Matsuda, H. Okawa, R. Miyamoto, S. Yamaguchi, T. Kojima, *Inorg. Chim. Acta* **2005**, *358*, 2489–2500.
- [18] a) C. H. Kirksey, P. Hambright, C. B. Storm, *Inorg. Chem.* **1969**, *8*, 2141–2144; b) C. H. Kirksey, P. Hambright, *Inorg. Chem.* **1970**, *9*, 958–960.
- [19] W. Jentzen, I. Turowska-Tyrk, W. R. Scheidt, J. A. Shelnut, *Inorg. Chem.* **1996**, *35*, 3559–3567.
- [20] M. J. Frisch, G. W. Trucks, H. B. Schlegel, G. E. Scuseria, M. A. Robb, J. R. Cheeseman, J. A. Montgomery, J. T. Vreven, K. N. Kudin, J. C. Burant, J. M. Millam, S. S. Iyengar, J. Tomasi, V. Barone, B. Mennucci, M. Cossi, G. Scalmani, N. Rega, G. A. Petersson, H. Nakatsuji, M. Hada, M. Ehara, K. Toyota, R. Fukuda, J. Hasegawa, M. Ishida, T. Nakajima, Y. Honda, O. Kitao, H. Nakai, M. Klene, X. Li, J. E. Knox, H. P. Hratchian, J. B. Cross, C. Adamo, J. Jaramillo, R. Gomperts, R. E. Stratmann, O. Yazyev, A. J. Austin, R. Cammi, C. Pomelli, J. W. Ochterski, P. Y. Ayala, K. Morokuma, G. A. Voth, P. Salvador, J. J. Dannenberg, V. G. Zakrzewski, S. Dapprich, A. D. Daniels, M. C. Strain, O. Farkas, D. K. Malick, A. D. Rabuck, K. Raghavachari, J. B. Foresman, J. V. Ortiz, Q. Cui, A. G. Baboul, S. Clifford, J. Cioslowski, B. B. Stefanov, G. Liu, A. Liashenko, P. Piskorz, I. Komaromi, R. L. Martin, D. J. Fox, T. Keith, M. A. Al-Laham, C. Y. Peng, A. Nanayakkara, M. Challacombe, P. M. W. Gill, B. Johnson, W. Chen, M. W. Wong, C. Gonzalez, J. A. Pople, *Gaussian 03, Revision C.02*, Gaussian, Inc., Wallingford, CT, **2004**.
- [21] *CrystalStructure 3.7.0, Crystal Structure Analysis Package*, Rigaku and Rigaku/MS, The Woodlands, TX 77381, USA, **2000–2005**.
- [22] G. M. Sheldrick, *SHELXL-97, Program Suite for the Solution and Refinement of Crystal Structures from Diffraction Data*, University of Göttingen, Germany, **1997**.
- [23] A. L. Spek, *J. Appl. Crystallogr.* **2003**, *36*, 7–13.

Received: October 22, 2008

Published Online: January 15, 2009